Antidepressant-Like Effects of Cortical Deep Brain Stimulation Coincide with Pro-Neuroplastic Adaptations of Serotonin Systems

Supplemental Information

Supplementary Methods and Materials

Mice

To generate Pet1-tdTomato mice, BAC transgenic *Pet1-Cre* mice (*B6.Cg-Tg(Fev-cre)*1Esd/J; JAX stock number 012712) (1) were crossed to floxed-stop controlled *tdTomato* (RFP variant) mice (*B6.Cg-Gt(ROSA)26Sor*$^{tm9(CAG\text{-}tdTomato)Hze}$*/J*; JAX stock number 007908) (2) to achieve fluorescent labeling of *Cre* containing cells.

Social Defeat and Social Interaction Testing

For 10 consecutive days, experimental mice were exposed to brief (5 min) physical encounters with an unfamiliar trained CD1 aggressor followed by overnight protected sensory contact with the aggressor through a perforated plexiglass partition. Control (undefeated) animals were housed in identical cages with another mouse from the same genotype and handled daily.

For social interaction testing, mice were placed in an open field arena with a small 10 x 6 cm wire mesh target box positioned on one side of the arena. During the first 2.5 minute trial ("Target Absent"), the mouse was allowed to freely explore the arena with the empty box. During the second 2.5 minute trial ("Target Present"), the mouse freely explored the arena while the target box was occupied by an unfamiliar CD1 aggressor. Video-tracking software (Cleversys, Reston, VA) was used to measure the time each mouse spent in the "interaction zone", a 14 x 26 cm rectangle surrounding the target box, along with total distance traveled. The

social interaction ratio (IR) was calculated as the percentage time spent in the interaction zone in the target-present condition relative to the target-absent condition. Classification as susceptible (IR < 100) and resilient (IR ≥ 100) was conducted as previously reported (3,4).

Histology and Immunohistochemistry

To determine electrode placements, 30 μm thick coronal ventromedial prefrontal cortex (vmPFC) slices were stained with hematoxylin and imaged on a stereoscope by a blinded experimenter.

For immunohistochemistry experiments, the following primary antibodies were applied to samples overnight at 4°C: rabbit anti-c-Fos (Santa Cruz Biotechnology, 1:1000), goat anti-PSD-95 (Abcam ab12093, 1:500) and chicken anti-GFP (AvesLab, 1:1000). Secondary antibodies (Alexa Fluor 647 or DyLight 649 fluorophores from Jackson ImmunoResearch Laboratories) were applied for 2 hours at 25°C. Slides were imaged at 200x magnification on a Leica TCS SPII Confocal Microscope and c-Fos^{+} nuclei or PSD-95 puncta were counted manually by a blinded experimenter using Leica LAS AF software. c-Fos nuclei were counted in the vmPFC, anterior piriform cortex, dentate gyrus, lateral habenula, basolateral amygdala, and dorsal raphe nucleus (DRN) at regions specified by the Paxinos Mouse Brain Atlas (5). Due to the presence of contralateral vmPFC activation, c-Fos nuclei in all regions were counted in both the ipsilateral and contralateral sides to the stimulation region and summed. Identified PSD-95 puncta with a diameter of under 30 nm were excluded from the analyses, consistent with typical PSD-95 puncta size minima (6).

Whole-cell Electrophysiology

Brain slices were prepared as previously described (7-9). The 200 µm coronal slices containing DRN were placed in artificial cerebrospinal fluid (aCSF) (in mM, NaCl 124, KCl 2.5, NaH_2PO_4 1.25, $MgSO_4$ 2.0, $CaCl_2$ 2.5, dextrose 10, $NaHCO_3$ 26) at 37°C, and aerated with 95% O_2/5% CO_2. After one hour, slices were kept at room temperature. Tryptophan (2.5 mM) was included in the holding chamber to maintain 5-HT synthesis, but was not in the aCSF perfusing the slice in the recording chamber. Individual slices were placed in a recording chamber (Warner Instruments, Hamden, CT) and perfused with aCSF at 2 mL/min maintained at 32°C by an in-line solution heater (TC-324, Warner Instruments). Neurons were visualized using a Nikon E600 upright microscope fitted with a 60X water immersion objective and targeted under DIC or fluorescent filters. Resistance of electrodes was about 8-10 MOhms when filled with a recording solution composed of (in mM) K-gluconate (130), NaCl (5), Na phosphocreatine (10), $MgCl_2$ (1), EGTA (0.02), HEPES (10), MgATP (2) and Na_2GTP (0.5) with 0.1% biocytin and a pH of 7.3. Whole-cell recordings were obtained using a Multiclamp 700B amplifier (Molecular Devices, Sunnyvale, CA). Cell characteristics were recorded using current clamp techniques as previously described (4,7). Signals were collected and stored using Digidata 1320 analog-to-digital converter and pClamp 9.0 software (Molecular Devices). Collection of inhibitory postsynaptic current (IPSC) data was performed as previously described (9) with bath application of 20 µM DNQX to block AMPA/Kainate synaptic activity. Frequency of excitatory postsynaptic potential (EPSC) activity was determined by subtracting IPSC frequency from the baseline frequency. All drugs were made in stock solutions, diluted on the day of the experiment and added directly to the ACSF.

Electrophysiology Data Analysis

Cellular characteristics were analyzed using Clampfit 9.0 (Molecular Devices). Synaptic properties were analyzed using MiniAnalysis (Synaptosoft, Decatur, GA) as previously described (9,10). Frequency-intensity plots were generated by measuring the number of action potentials generated by depolarizing current steps ranging from 0 to 120 pA in 20 pA increments. Average firing rate for each condition was determined by the number of action potentials generated over the 500 ms current pulse. Synaptic events were analyzed using parameters optimized for each cell with the detection threshold set beyond the maximum values of the all-points noise histogram for a portion of the trace containing no detectable synaptic events. This threshold generally ranged from 5 to 8 pA. MiniAnalysis generated a summary table containing the mean and median values for the frequency, amplitude, rise time (10-90%), decay time and event half width (50%). For each cell, at least 200 events were chosen at random and manually filtered to exclude multiple peaks then combined to obtain an averaged EPSC or IPSC for each cell to obtain values for decay time, event area, and event time half-width. The Kolmogorov-Smirnov test was used to determine whether the histograms and cumulative probability plots of the synaptic activity characteristics were different between each group. Additional statistical analysis is described in the Statistical Methods section of the Methods and Materials section in the main paper. Data reported are means ± SEM.

Morphometric Analyses of Somatodendritic Structure and Axonal Boutons of 5-HT Neurons

For analyses of somatodendritic structure, neurons were filled with 1% biocytin during whole-cell recording and were processed for immunohistochemical detection. A 20x objective

lens and optical z-slices of 0.8 µm thickness were used to capture the entire extent of the dendritic tree. Confocal stacks were then analyzed using Neurolucida (version 9; MBF Bioscience). The cell soma and dendrites were traced using the Autoneuron feature and then manually edited by a blinded experimenter if necessary to ensure accurate tracing. Sholl analysis was performed using radial shells at 20 µm intervals.

For morphometric analyses of presynaptic boutons, we used a conditional viral vector AAV2/9.CMV.Flex.Synaptophysin-Venus.WPRE.hGH (a kind gift of Anton Maximov, Scripps, La Jolla, CA) that restricts expression of SynP-Venus to Cre-recombinase-expressing neurons (11). The vector was packaged into viral particles to a titer of $4*10^{13}$ CG/ml by the vector core of the University of Pennsylvania. Seven days prior to the beginning of chronic social defeat stress, the AAV vector was injected stereotaxically into the DRN (from lambda, in mm: 0.0 AP, +0.8 ML, -3.3 DV, 15° angle) of *Pet1-tdTomato* mice, which express the Cre-recombinase selectively in serotonin neurons (1). Synaptophysin is a protein integral to synaptic vesicles that has been widely used both *in vitro* (12) and *in vivo* (13) after transient viral overexpression (14) or constitutive expression in transgenic animals (13) to identify functional synapses and assess their plasticity. Previous studies have shown that SynP transgenes tagged with variants of GFP adequately co-localize with endogenous synaptic proteins and identify functional synapses with 90% accuracy, without altering presynaptic function (13,15,16). Time-lapse studies in live rodent neocortex showed that axonal boutons labeled with SynP are dynamic and display a turnover of 7% per day (17). Studies also report fluctuations in the volume of stable axonal boutons. Activity-dependent increases in density and size of SynP-eGFP labeled varicosities have been validated as quantitative dynamic index for synaptic strength in neurons (18).

To visualize boutons, slices were imaged at 630x magnification with an additional 3.5x digital zoom. Serotonergic axons were manually traced on Leica LAS AF software using tdTomato as a guide. Axons for tracing were selected randomly by an experimenter blinded to the condition of each mouse. Each trace generated a line measurement plot for Venus fluorescence intensity (**Figure S3**). An automated bouton detection and measurement algorithm was developed in MATLAB and validated based on parallel manual analysis of a pilot dataset. Based on pilot data, boutons were defined as having a minimal intensity of 95 pixel intensity units (2 times the intensity of the maximum noise observed) and a minimal length of 0.1 µm, which is similar to minima observed in electron microscopy studies of CA3-CA1 axons (19). Objects detected outside these boundaries were filtered out as artifacts. Bouton length was measured at the intensity threshold (**Figure S3**). Bouton density for an axon was calculated as the total number of boutons along the axon divided by the total axon length.

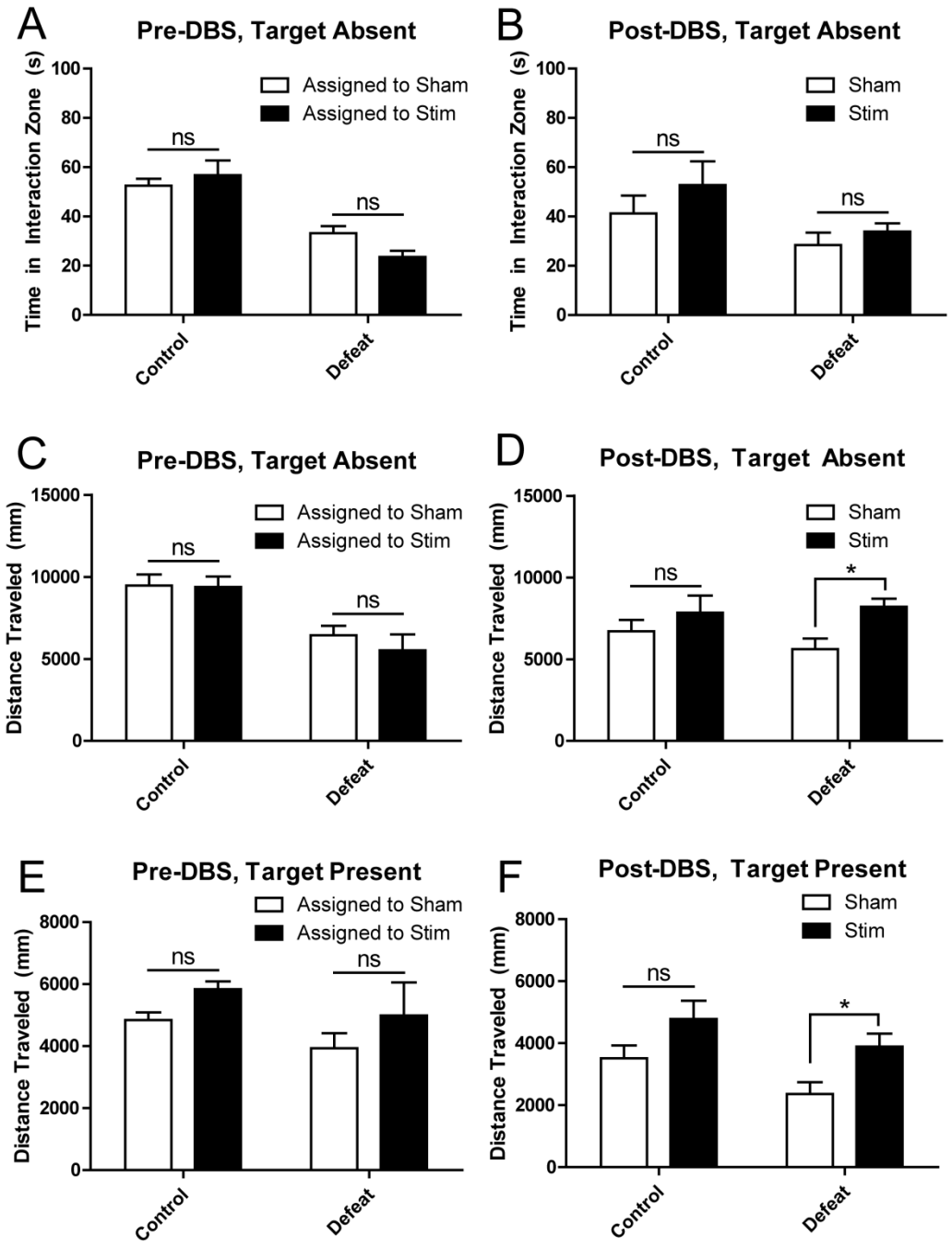

Figure S1. Supplementary DBS behavioral data. (**A**-**B**) DBS does not affect interaction time in the absence of a social target. (**C**-**F**) DBS increases total distanced traveled regardless of target presence. *$p < 0.05$. DBS, deep brain stimulation.

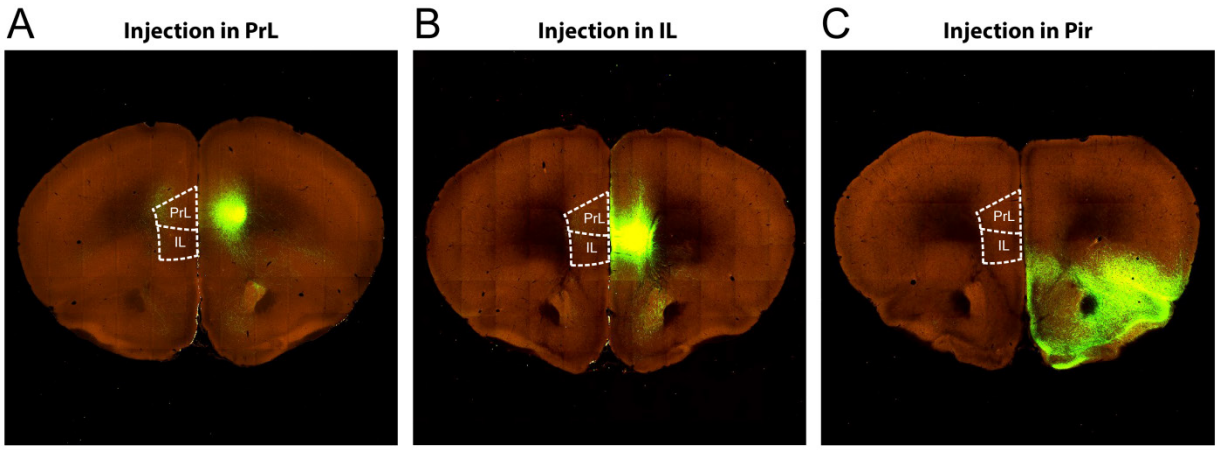

Figure S2. The anterior piriform cortex (Pir) projects to the ventral infralimbic cortex (IL), but does not receive projections from the ventromedial prefrontal cortex. (A) Prelimbic cortex (PrL) injection does not result in labeled fibers in the Pir. **(B)** IL injection does not result in labeled fibers in the Pir. **(C)** Pir injection results in labeled fibers in the IL. Images obtained from the Allen Institute for Brain Science website at www.alleninstitute.org. Image credit: Allen Institute for Brain Science

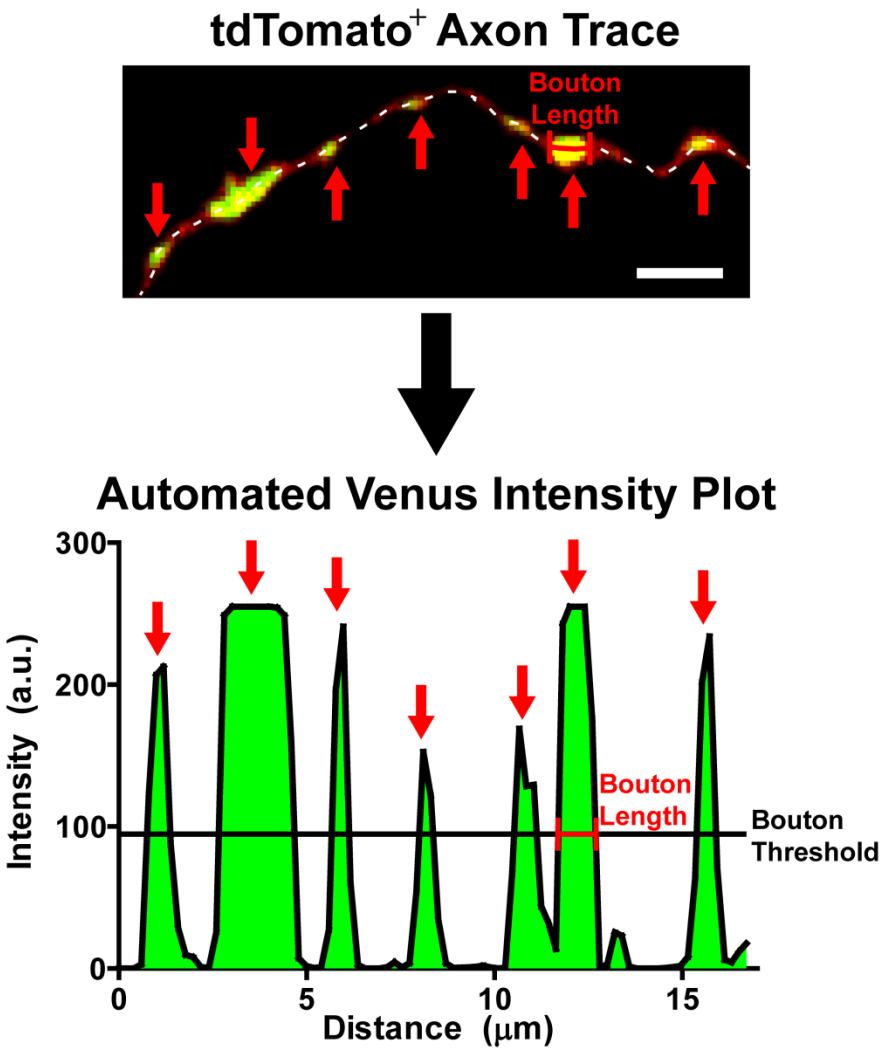

Figure S3. Methodology of bouton analysis and quantification. Axons originating from dorsal raphe nucleus 5-HT neurons were identified from native tdTomato fluorescence and Venus$^+$ boutons labeled by immunohistochemistry. Axons were manually traced along tdTomato fluorescence (top panel, dashed white line) using LAS AF software to generate a Venus fluorescence intensity plot. Venus$^+$ boutons generated large fluorescent peaks, which were detected by thresholding (bottom panel). Fluorescence intensity analyses allowed for measurement of bouton length (width of peak at threshold) and bouton density (number of discrete peaks above threshold divided by total length of trace). Scale bar: 2 μm.

Supplemental References

1. Scott MM, Wylie CJ, Lerch JK, Murphy R, Lobur K, Herlitze S, *et al.* (2005): A genetic approach to access serotonin neurons for in vivo and in vitro studies. *Proc Natl Acad Sci U S A.* 102: 16472-16477.

2. Madisen L, Zwingman TA, Sunkin SM, Oh SW, Zariwala HA, Gu H, *et al.* (2010): A robust and high-throughput Cre reporting and characterization system for the whole mouse brain. *Nat Neurosci.* 13: 133-40.

3. Golden SA, Covington HE, Berton O, Russo SJ (2011): A standardized protocol for repeated social defeat stress in mice. *Nat Protoc.* 6: 1183-91.

4. Espallergues J, Teegarden S, Veerakumar A, Boulden J, Challis C, Jochems J, *et al.* (2012): HDAC6 regulates glucocorticoid receptor signaling in serotonin pathways with critical impact on stress resilience. *J Neurosci.* 32: 4400-4416.

5. Paxinos G, Franklin K (2001): *The Mouse Brain in Stereotaxic Coordinates, Second Edition*. San Diego: Academic Press.

6. Dumitriu D, Berger SI, Hamo C, Hara Y, Bailey M, Hamo A, *et al.* (2012): Vamping: stereology-based automated quantification of fluorescent puncta size and density. *J Neurosci Methods.* 209: 97-105.

7. Crawford LK, Craige CP, Beck SG (2010): Increased intrinsic excitability of lateral wing serotonin neurons of the dorsal raphe: a mechanism for selective activation in stress circuits. *J Neurophysiol.* 103: 2652-2663.

8. Calizo LH, Akanwa A, Ma X, Pan Y, Lemos JC, Craige C, *et al.* (2011): Raphe serotonin neurons are not homogenous: electrophysiological, morphological and neurochemical evidence. *Neuropharmacology* 61: 524-43.

9. Crawford LK, Rahman SF, Beck SG (2013): Social stress alters inhibitory synaptic input to distinct subpopulations of raphe serotonin neurons. *ACS Chem Neurosci.* 4: 200-209.

10. Crawford LK, Craige CP, Beck SG (2011): Glutamatergic input is selectively increased in dorsal raphe subfield 5-HT neurons: role of morphology, topography and selective innervation. *Eur J Neurosci.* 34: 1794-1806.

11. Atasoy D, Aponte Y, Su H, Sternson S (2008): A FLEX switch targets Channelrhodopsin-2 to multiple cell types for imaging and long-range circuit mapping. *J Neurosci.* 28: 7025-30.

12. Kelsch W, Sim S, Lois C (2010): Watching synaptogenesis in the adult brain. *Annu Rev Neurosci.* 33: 131-149.

13. Li L, Tasic B, Micheva KD, Ivanov VM, Spletter ML, Smith SJ, Luo L (2010): Visualizing the distribution of synapses from individual neurons in the mouse brain. *PloS One* 5: e11503.

14. Grinevich V (2005): Monosynaptic pathway from rat vibrissa motor cortex to facial motor neurons revealed by lentivirus-based axonal tracing. *J Neurosci.* 25: 8250-8258.

15. Gogolla N, Galimberti I, Caroni P (2007): Structural plasticity of axon terminals in the adult. *Curr Opin Neurobiol.* 17: 516-524.

16. Jin I, Udo H, Hawkins R (2011): Rapid increase in clusters of synaptophysin at onset of homosynaptic potentiation in Aplysia. *Proc Natl Acad Sci U S A.* 108: 11656-61.

17. Stettler DD, Yamahachi H, Li W, Denk W, Gilbert CD (2006): Axons and synaptic boutons are highly dynamic in adult visual cortex. *Neuron* 49: 877-87.

18. Zhang Z, Kang JI, Vaucher E (2011): Axonal varicosity density as an index of local neuronal interactions. *PLoS One.* 6: e22543.

19. Shepherd G, Harris K (1998): Three-dimensional structure and composition of CA3-->CA1 axons in rat hippocampal slices: implications for presynaptic connectivity and compartmentalization. *J Neurosci.* 18: 8300-10.